J KAU: Earth Sci., **vol. 1**, pp. 27-60 (1408A.H./1988A.D.)

Petroleum Generation and Maturation of the Arabian Gulf Region

I.A. SAIL and K. MAGARA
Department of Petroleum Geology, Faculty of Earth Sciences,
King Abdulaziz University, Jeddah, Saudi Arabia.

ABSTRACT. The result of application of Lopatin's and Waples' methods on generation and maturation of petroleum in the Arabian region proves that the Permian and Triassic sedimentary rocks are possible sources for only gas and the Tertiary sediments have generated only heavy oils (immature). However, the study of the Jurassic and Cretaceous source rocks indicates that they are the main hydrocarbon generators with large areal distributions. The superposition of the existing oil and gas fields over the petroleum generation maps further confirms the above result.

Introduction

Vitrinite reflectance has been widely used as an index of the level of organic maturation, which is important in assessing the status of petroleum generation and maturation in source rocks. Figure 1 summarizes several maturation indices including vitrinite reflectance in relation to oil and gas generation (Dow 1977).

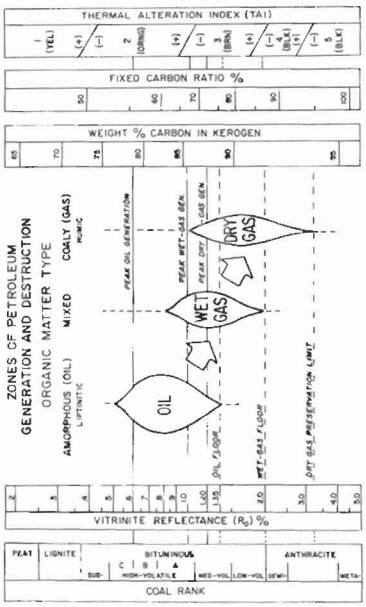

FIG. 1. Maturation indices including vitrinite reflectance, R_o, in relation to oil and gas generation (Dow 1977).

Because vitrinite reflectance values are measured using rock samples, proper estimate of organic maturation in the subsurface can only be made after drilling a well. However, in most exploration plays, it is desirable to have such an estimate before drilling. Both organic maturation and vitrinite reflectance are primarily controlled by temperature and duration of geologic time (Connan 1974). Therefore, it is possible to estimate the reflectance if a relationship among the reflectance, geologic age, and depth of burial (or temperature) in a study area is known. Figure 2 shows such an empirical relationship for the Gulf Coast sedimentary rocks (Dow 1978). This figure only represents an example of Gulf Coast, which was not used for the current study described in this paper.

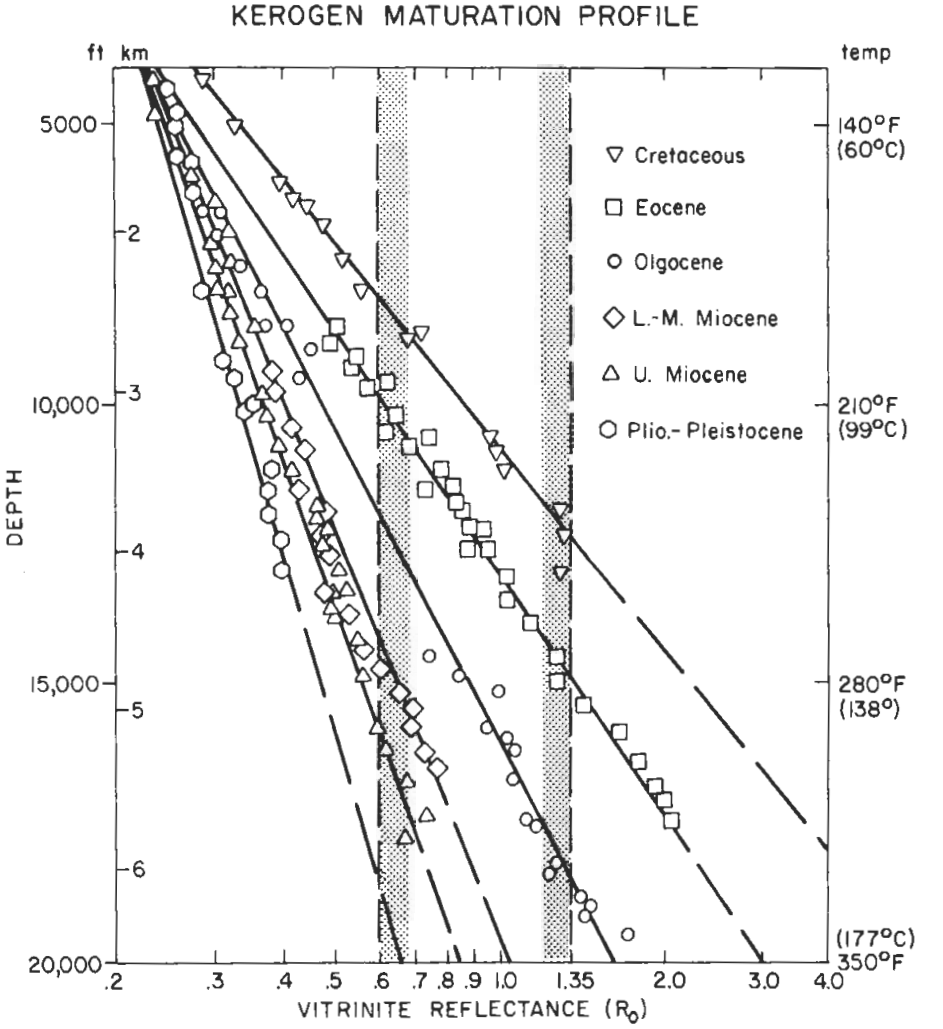

FIG. 2. Empirical relationship between vitrinite reflectance, R_o, and depth for the Gulf Coast sedimentary rocks (Dow 1978).

Where rates of sediment burial were relatively uniform throughout an entire geologic period, a plot of depth of a bed of known geologic age provides a reliable estimate of vitrinite reflectance such as in Fig. 2. However, if the rate of burial was significantly changed in the geological past, or if major erosional periods were involved, a reliable estimate cannot be made by simply plotting the depth or temperature value on a chart such as that of Fig. 2.

To make a proper estimate of vitrinite reflectance, the burial history and the time-temperature index of a given sedimentary rock must be estimated (Waples 1980). Based on Lopatin's (1971) fundamental concept, Waples stated that the time-temperature index (TTI) or the maturity indicator of a given sediment is given by the sum of the maturities acquired in each time-temperature index, or

$$TTI = \sum_{n\,min}^{n\,max} (\Delta t_n) \cdot (r^n) \qquad (1)$$

where Δt_n is the length of time spent by the sediment in the n *th* temperature interval, r^n is the temperature factor of the same interval shown in Table 1, and n max and n min are the n-values of the highest and lowest temperature intervals encountered.

TABLE 1. List of temperature interval, index value, n, and temperature factor, r^n, for calculation of time-temperature indices or integrals (TTI) (from Waples 1980).

Temperature interval (°C)	Index Value n	Temperature Factor r^n
10- 20	–8	2^{-8}
20- 30	–7	2^{-7}
30- 40	–6	2^{-6}
40- 50	–5	2^{-5}
50- 60	–4	2^{-4}
60- 70	3	2^{-3}
70- 80	–2	2^{-2}
80- 90	–1	2^{-1}
90-100	–0	1
100-110	1	2
110-120	2	2^2
120-130	3	2^3
130-140	m	2^m

Once the TTI value is calculated for a given sample, it can be converted to vitrinite reflectance, R_o, using Figure 3, which is a plot of Waples' correlation between TTI and R_o derived from 402 worldwide samples. In short, Waples' method is a method which combines Lopatin's theory and the true subsurface data obtained worldwide.

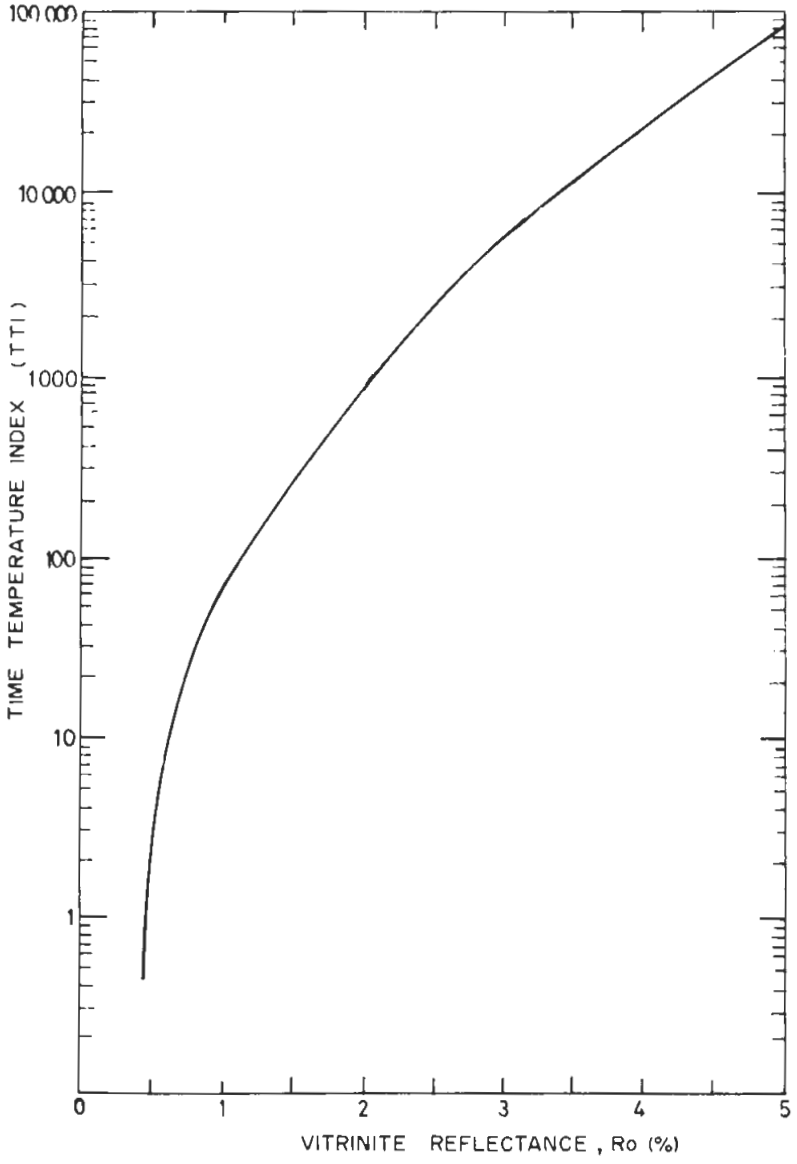

FIG. 3. Time-temperature index (TTI) and vitrinite reflectance, R_o, plot (Waples 1980).

Vitrinite reflectance is normally measured on the actual subsurface samples (cuttings or cores) by using a microscope. During the current study, such measurements were made on the samples from two oil fields in the Kingdom to document the validity of Waples' method described above. However, because of the confidential nature of the data, we are unable to show the result in this paper.

Vitrinite reflectance based on the actual subsurface samples can be estimated only in anticlinal areas, because virtually all the petroleum wells are drilled there. On the contrary, most petroleum is considered to have been originated from the synclinal areas because the synclines usually cover larger area and also are geochemically more mature. This is generally true, even if some vertical petroleum migration is involved along with the lateral migration. In short, vitrinite reflectance based on the actual samples does not represent the synclinal areas where most oil has been generated, because virtually no subsurface samples are available in the synclines.

There are also two other advantages of using Waples' method over the method based on the actual samples; 1. The former method can estimate the organic maturity of a bed at any stage in the geological past as well as at present. On the contrary, the latter method can estimate the maturity only at the present time. 2. The former method has greater chances of application, because it is simple and quick, and does not require a large number of confidential data.

As a matter of fact, at the Department of Petroleum Geology of the King Abdulaziz University, the authors had no other alternative but using Waples' method, because we are not allowed to show the result of the actual measurements of vitrinite reflectance in a printed form.

It is, however, always recommended to examine the results obtained by Waples' method using the actual samples in the region, even though such an examination or documentation can be made only for the anticlinal areas where the samples are available.

Although the validity of the vitrinite reflectance or Waples' method in general is not our main concern in this paper, the following point may be worthy for discussion. In the region, where most petroleum was derived from typical marine source material (e.g. alginite), the oil generation zone indicated by vitrinite would have little meaning, except that it may infer a possibility of generating oil. The actual amount of oil generated from the source rocks largely depends on the type and quantity of the proper organic matter in sediments.

Because of the above reason, the reader must consider the oil generation zone described in this paper as a zone with a mere possibility of generating oil. Despite the limitations and difficulties of both vitrinite reflectance and Waples' method, they have been quite widely used in many sedimentary basins of the world. One excellent example of such application in the study area was published by Ayres *et al.* (1982).

During the current study, the authors also faced other major difficulties related to

data 1. The only regional isopach maps available to us are those constructed by Kamen-Kaye in 1970, because more recent data have not been released to public on a regional basis. 2. The subsurface temperature values of various reservoirs were reported by Young *et al.* (1977). We had to use these values regionally because there was no other alternative. Hopefully in future, one may be able to improve the assessment of petroleum generation in the region, by the use of better temperature data.

In this region, the rate of burial had significantly changed in the geological past, as the result of regional tectonism. This situation is clearly shown in the burial history plots based on Kamen-Kaye's data (1970). However, the detailed discussion of the regional tectonic movement is outside the scope of this paper (see Powers *et al.* 1966, Baydoun and Dunnington 1975 and Murris 1980). Possible effect of erosion on maturation was not considered in this paper, because the erosional thicknesses in different areas in the region could not be estimated from the available data.

The possibility of vertical oil migration was discussed by various workers (Young *et al.* 1977, Ayres *et al.* 1982, and Ala 1982). The result of our study also suggests that such vertical migration would have happened.

Generation and Maturation of Petroleum in the Arabian Gulf Region

In 1970, Kamen Kaye published a paper entitled "Geology and Productivity of Persian Gulf Synclinorium", in which he collected data and constructed five regional isopach maps of the Permian, Triassic, Jurassic, Cretaceous, and Tertiary periods. These five isopach maps were chosen as basic data for the study of regional petroleum geology in this paper. Using these original isopach maps, a series of cumulative isopach maps (e.g. Permian plus Triassic, Permian plus Triassic plus Jurassic, etc) were constructed. Each isopach map or cumulative isopach map depicts the burial contour map of a layer at a given geologic stage. For example, Permian isopach map is the burial map of a layer at the base of the Permian section at the end of the Permian period (Fig. 8). The cumulative isopach map of Permian through Triassic is the burial map of a layer at the base of Permian section at the end of Triassic period (Fig. 9). In such constructions of the paleoburial maps, variation of paleo (depositional) water depth is not considered. Effect of sediment compaction and erosion are not considered either, on the assumption that it did not cause significant changes in the evaluation of hydrocarbon generation and maturation. A total of ten burial maps were constructed by this method in addition to the five original ones (Fig. 8-22).

Before mapping the regional oil maturation, fifteen locations were arbitrarily chosen for constructing burial history plots (see solid circles in Fig. 4 for locations). Note that these locations represent neither oil fields nor oil wells, but were selected arbitrarily or randomly. Although a large number of the burial history plots and the time-temperature tables were constructed for these locations, only those for three locations (6, 11 and 12 in Fig. 4) are shown as examples in this paper; they are Figures 5, 6, and 7 (burial history plots) and Tables 2, 3 and 4 (time-temperature data and calculated TTI and R_o).

TABLE 2. Calculation of time-temperature index (TTI) and vitrinite reflectance, R_o, for the Location No. 6 at bases of Permian, Triassic, Jurassic, Cretaceous and Tertiary periods, respectively.

Temperature interval C	Rate of reaction r	Time Interval Δt	r.Δt	TTI	R_o	Remarks (R_o)
Permian						
30- 40	1/128	30	0.23	0.23	0.43	0.445
40- 50	1/64	29	0.45	0.68	0.46	
50- 60	1/32	21	0.66	1.34	0.48	0.485
60- 70	1/16	32	2	3.34	0.501	
70- 80	1/8	40	5	8.34	0.57	0.58
80- 90	1/4	6	1.5	9.84	0.59	
90-100	1/2	9	4.5	14.34	0.63	
100-110	1	11	11	25.34	0.75	
110-120	2	10	20	45.34	0.8	
120-130	4	10	40	85.34	1.1	
130-140	8	10	80	165.34	1.3	1.3
140-150	16	8	80	245.34	1.5	
150-160	32	9	288	533.34	1.8	
160-170	64	8	512	1045.34	2.08	
170-180	128	9	1152	2197.34	2.45	
180-190	256	8	2048	4245 .34	2.75	
190-200	512	10	5120	9365.34	3.45	
200-210	1024	9	9216	18581.34	3.85	
210-220	2048	1	2048	20629.34	4.00	4.00
Triassic						
30- 40	1/128	15	0.12	0.12	0.41	
40- 50	1/64	19	0.30	0.42	0.44	0.45
50- 60	1/32	38	1.19	1.61	0.47	
60- 70	1/16	34	2.13	3.74	0.51	0.53
70- 80	1/8	14	1.75	5.49	0.55	
80- 90	1/4	11	2.75	8.24	0.59	
90-100	1/2	9	4.5	12.74	.62	
100-110	1	12	12	24.74	0.74	
110-120	2	10	20	44.74	0.87	0.93
120-130	4	10	40	84.74	1.07	
130-140	8	10	80	164.74	1.3	
140-150	16	8	148	312.74	1.6	
150-160	32	8	256	568.74	1.75	
160-170	64	9	576	1144.74	2.07	
170-180	128	8	1024	2168.74	2.45	
180-190	256	9	2304	4472.74	2.88	
190-200	512	8	4096	8568.74	3.3	3.3

Temperature interval °C	Rate of reaction r	Time Interval Δt	r.Δt	TTI	R_o	Remarks (R_o)
Jurassic						
30- 40	1/128	42	0.33	0.33	0.44	0.45
40- 50	1/64	36	0.56	0.89	0.46	
50- 60	1/32	9	0.28	1.17	0.47	
60- 70	1/16	9	0.56	1.73	0.48	
70- 80	1/8	8	1	2.73	0.5	
80- 90	1/4	10	2.25	4.98	0.54	
90-100	1/2	8	4	8.98	0.6	0.6
100-110	1	10	10	18.98	0.7	
110-120	2	8	16.	34.98	0.82	
120-130	4	9	36	70.98	1.01	
130-140	8	8	64	134.98	1.22	
140-150	16	8	80	214.98	1.41	
150-160	32	9	288	502.98	1.77	
160-170	64	9	576	1078.98	2.08	
170-180	128	11	1408	2486.98	2.5	2.5
Cretaceous						
30- 40	1/128	7	0.05	0.05	–	
40- 50	1/64	10	0.16	0.21	0.45	
50- 60	1/32	11	0.34	0.55	0.46	
60- 70	1/16	9	0.56	1.11	0.48	
70- 80	1/8	11	1.38	2.49	0.5	0.52
80- 90	1/4	10	2.5	4.99	0.54	
90-100	1/2	8	4	8.99	0.59	
100-110	1	9	9	17.99	0.7	
110-120	2	9	18	35.99	.8	
120-130	4	8	32	67.99	1	
130-140	8	8	64	131.99	1.15	
140-150	16	9	90	221.99	1.4	
150-160	32	11	352	573.99	1.8	1.8
Tertiary						
30- 40	1/128	6	0.05	0.05	–	
40- 50	1/64	8	0.13	0.18	0.45	
50- 60	1/32	9	0.28	0.46	0.46	
60- 70	1/16	8	0.5	0.96	0.48	
70- 80	1/8	8	1	1.96	0.49	
80- 90	1/4	9	2.25	4.21	0.53	
90-100	1/2	8	4	8.21	0.58	
100-110	1	8	8	16.21	0.65	0.65

For symbols, refer to text.

TABLE 3. Calculation of time-temperature index (TTI) and vitrinite reflectance, R_o, for the Location No. 11 at bases of Permian, Triassic, Jurassic, Cretaceous and Tertiary periods respectively.

Temperature interval °C	Rate of reaction r	Time Interval Δt	r.Δt	TTI	R_o	Remarks (R_o)
Permian						
30- 40	1/128	48	0.375	0.375	0.45	0.45
40- 50	1/64	21	0.328	0.703	0.47	0.48
50- 60	1/32	30	0.938	1.641	0.49	
60- 70	1/16	51	3.188	4.829	0.53	0.57
70- 80	1/8	29	3.625	8.454	0.58	
80- 90	1/4	19	4.75	13.204	0.6	
90-100	1/2	18	9	22.204	0.734	0.8
100-110	1	23	23	45.204	0.86	
110-120	2	28	56	101.204	1.13	
120-130	4	23	92	193.204	1.46	1.46
Triassic						
30- 40	1/128	16	0.125	0.125	0.4	
40- 50	1/63	22	0.344	0.469	0.45	0.45
50- 60	1/32	42	1.323	1.792	0.49	0.51
60- 70	1/16	35	2.188	3.98	0.52	
70- 80	1/8	19	2.375	6.355	0.56	
80- 90	1/4	20	5.	11.355	0.6	.72
90-100	1/2	20	40	51.355	0.92	
100-110	1	28	28	79.355	1.05	
110-120	2	30	60	139.355	1.7	1.7

Temperature interval °C	Rate of reaction r	Time Interval Δt	r.Δt	TTI	R_o	Remarks (R_o)
Jurassic						
30- 40	1/128	30	0.234	0.234	0.44	
40- 50	1/64	40	0.625	0.859	0.48	0.482
50- 60	1/32	22	0.688	1.547	0.485	
60- 70	1/16	18	1.125	2.672	0.5	
70- 80	1/8	20	2.5	5.172	0.54	0.54
80- 90	1/4	26	6.5	11.672	0.6	
90-100	1/2	26	13	24.672	0.72	
100-110	1	12	12	36.672	0.84	.84
Cretaceous						
30- 40	1/128	14	0.929	0.929	0.480	
40- 50	1/64	18	0.281	1.21	0.485	
50- 60	1/32	20	0.625	1.835	0.495	
60- 70	1/16	23	1.437	3.273	0.505	0.497
70- 80	1/8	27	3.375	6.648	0.56	
80- 90	1/4	18	4.5	11.148	0.62	0.62
Tertiary						
30- 40	1/128	19	0.148	0.148	0.43	
40- 50	1/64	27	0.422	0.57	0.46	
50- 60	1/32		0.563	1.133	0.48	0.48
60- 70	1/16	–	–	–	–	–
70- 80	1/8	–	–	–	–	–

For symbols, refer to text.

TABLE 4. Calculation of time-temperature index (TTI) and vitrinite reflectance, R_o, for the Location No. 12 at bases of Permian, Triassic, Jurassic, Cretaceous and Tertiary periods respectively.

Temperature interval °C	Rate of reaction r	Time Interval Δt	r.Δt	TTI	R_o	Remarks (R_o)
Permian						
30- 40	1/128	35	0.273	0.273	–	0.48
40- 50	1/64	29	0.453	0.726	0.48	0.484
50- 60	1/32	24	0.75	1.476	0.485	
60- 70	1/16	31	1.9375	3.4135	0.5	
70- 80	1/8	32	4	7.4135	0.58	0.6
80- 90	1/4	17	4	11.6635	0.62	
90-100	1/2	11	5.5	17.1635	0.7	
100-110	1	11	11	28.1635	0.8	
110-120	2	11	22	50.1635	0.92	
120-130	4	12	48	98.1635	1.1	1.15
130-140	8	12	96	194.1635	1.35	
140-150	16	14	224	418.1635	1.7	
150-160	32	15	480	898.1635	2.	
160-170	64	25	1600	2498.1635	2.5	
170-180	128	11	1408	3906.1635	2.75	2.75
Triassic						
30- 40	1/128	18	0.1406	0.1406	–	0.48
40- 50	1/64	23	0.3594	0.5	–	
50- 60	1/32	33	1.031	1.531	0.49	
60- 70	1/16	31	1.9375	3.4685	0.5	0.53
70- 80	1/8	16	2	5.4685	0.55	
80- 90	1/4	11	2.75	8.2185	0.6	
90-100	1/2	10	5	13.2185	0.65	
100-110	1	12	12	25.2185	0.76	
110-120	2	10	20	45.2185	0.9	1.1
120-130	4	14	56	101.2185	1.15	
130-140	8	14	112	213.2185	1.4	
140-150	16	13	208	421.2185	1.7	
150-160	32	16	512	933.2185	2.04	
160-170	64	11	704	1637.2185	2.25	2.25
Jurassic						
30- 40	1/128	24	0.1875	0.1875	–	0.47
40- 50	1/64	31	0.4844	0.6719	0.46	
50- 60	1/32	24	0.75	1.4219	0.48	
60- 70	1/16	10	0.625	2.0469	0.498	
70- 80	1/8	11	1.375	3.4219	0.5	
80- 90	1/4	11	2.75	6.1719	0.56	
90-100	1/2	11	5.5	11.6719	0.62	0.7
100-110	1	12	12	23.6719	0.75	
110-120	2	14	28	51.6719	0.92	
120-130	4	15	60	111.6719	1.15	
130-140	8	14	112	223.6719	1.4	
140-150	16	17	272	495.6719	1.7	1.7
Cretaceous						
30- 40	1/128	8	0.0625	0.0625	–	0.53
40- 50	1/64	11	0.1719	0.23244	–	
50- 60	1/32	11	0.3437	0.5781	–	
60- 70	1/16	10	0.625	1.2031	0.48	
70- 80	1/8	11	1.375	2.5781	0.5	
80- 90	1/4	13	3.25	5.8281	0.55	
90-100	1/2	13	6.5	12.3281	0.64	
100-110	1	15	15	27.3281	0.8	
110-120	2	15	30	57.3281	0.95	
120-130	4	13	52	109.3281	1.15	1.15
130-140	8	8	–	–	–	
Tertiary						
30- 40	1/128	10	0.0781	0.0781	–	
40- 50	1/64	14	0.2187	0.2968	–	
50- 60	1/32	16	0.5	0.7968	–	
60- 70	1/16	14	0.815	1.6718	0.49	
70- 80	1/8	10	1.25	2.9218	0.5	
80- 90	1/4	–	–	–	–	

For symbols, refer to text.

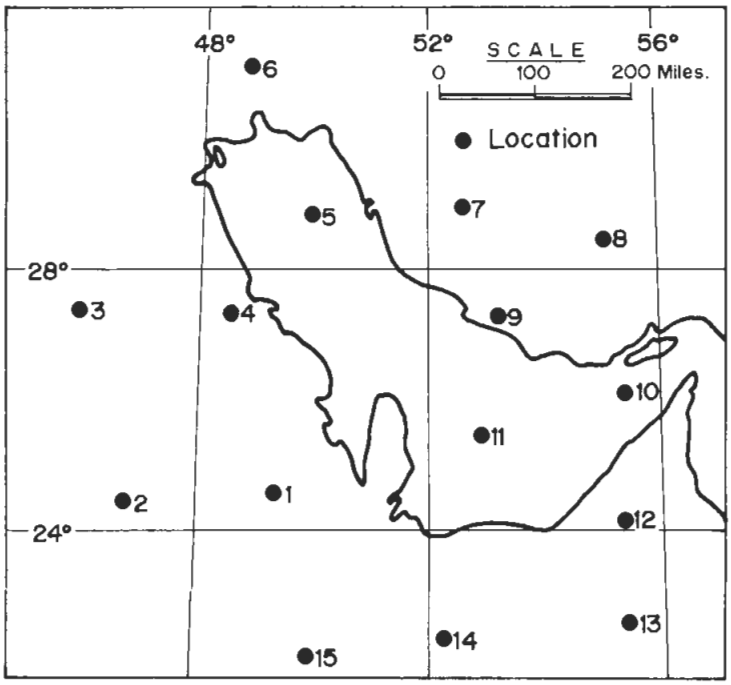

FIG. 4. Map showing arbitrarily selected locations in the Arabian Gulf region for burial history plots.

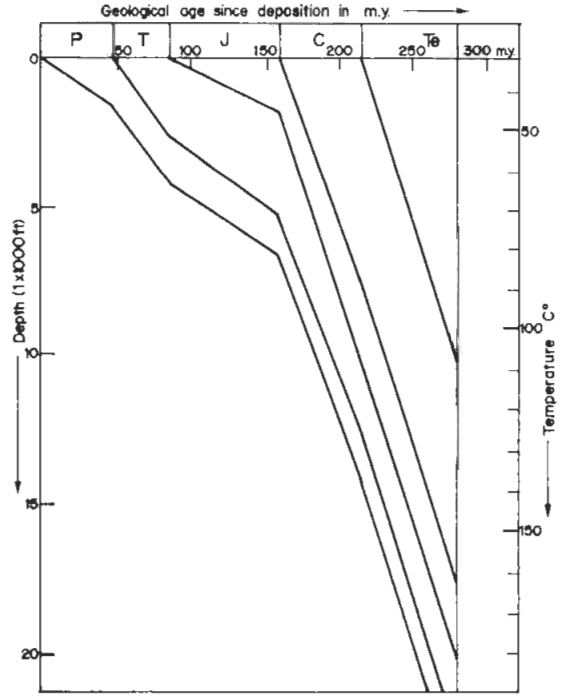

FIG. 5. Burial history plots for location No. 6 (refer to Fig. 4 for location): P = Permian, T = Triassic, J = Jurassic, C = Cretaceous, and Te = Tertiary.

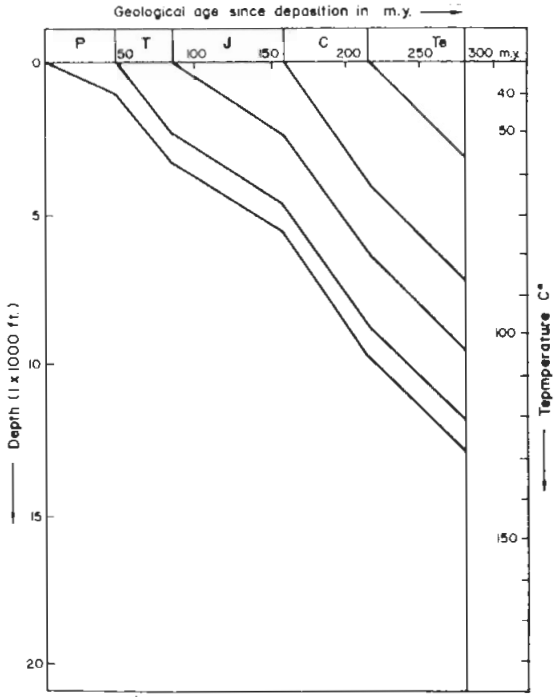

FIG. 6. Burial history plots for location No. 11 (refer to Fig. 4 for location). For the symbols, refer to caption of Fig. 5.

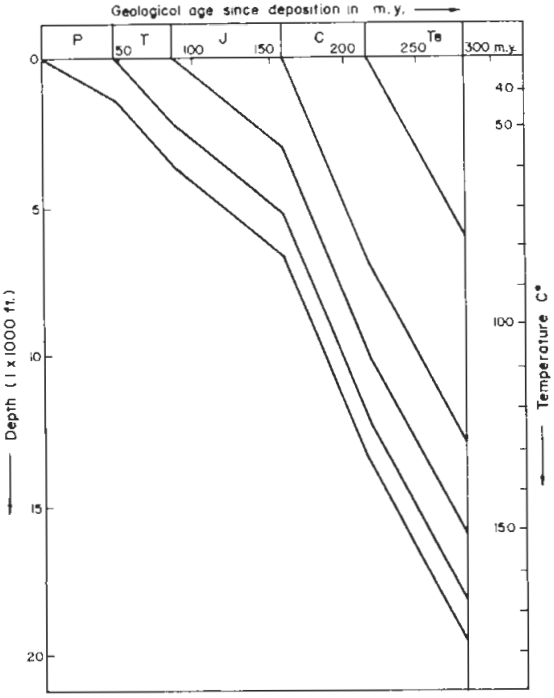

FIG. 7. Burial history plots for location No. 12 (refer to Fig. 4 for location). For the symbols, refer to caption of Fig. 5.

Burial and Petroleum Generation of a Bed at Permian Base

1. Burial Map of Base of Permian at end of Permian Period (Fig. 8)

a) Sedimentation and Paleostructure

Sedimentation at this stage spread over the entire Arabian Gulf region. Thickest areas of sedimentation occurred in the northwestern and eastern parts of the region (A_1 and A_2 in Fig. 8), where the thickness amounts to about 1,500 ft.

It is interpreted that subsidence reached its maximum in those parts of the region. On the other hand, areas of relatively thin sedimentation existed in the northern and southern parts of the region (B_1 and B_2 in Fig. 8), where burial is also considered to be relatively shallow. Based on the above observations and interpretations, compaction fluid (in this early stage of burial, mostly water) should have moved from relatively deep subsidence areas to shallow ones.

b) Petroleum Generation and Maturation

As depicted in Figure 8, the calculated vitrinite reflectance, R_o, ranges from 0.43 to 0.46%. This suggests that there was virtually no chance for oil generation at this stage.

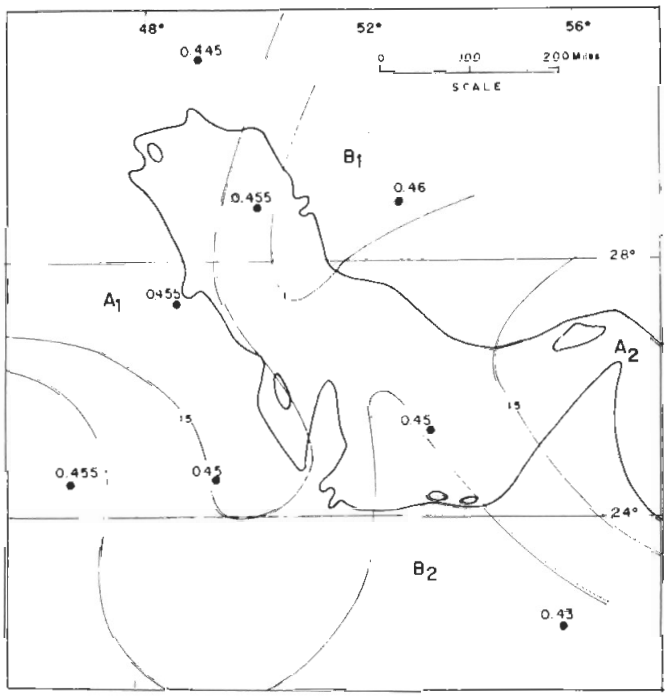

FIG. 8. Burial map of base of Permian at end of Permian period. Numbers on contour lines indicate burial depth or thickness in thousand feet (e.g. 1.5 = 1500 ft). Number on each location shows calculated vitrinite reflectance, R_o. For other symbols, refer to text. Original data derived from Kamen-Kaye (1970).

2. *Burial Map of Base of Permian at end of Triassic Period (Fig. 9)*

a) Sedimentation and Paleostructure

Figure 9 shows the thickest areas in the northwestern and eastern parts of the Arabian Gulf region (see A_1 and A_2) whereas the thinnest sedimentation occurred in the northern and southern parts of the region (B_1 and B_2 in Fig. 9).

The thickest as well as thinnest areas occurred in the same general areas as those in the previous stage (Fig. 9). This suggests that similar subsiding and relative uplifting patterns continued from Permian to the end of Triassic.

b) Petroleum Generation and Maturation

The calculated vitrinite reflectance, R_o, as shown in (Fig. 9), varies from 0.47 at the thin areas to 0.56% at the maximum geosynclines. This suggests that there was still no chance for major oil generation, where the compaction fluid might have contained slight amounts of heavy oil.

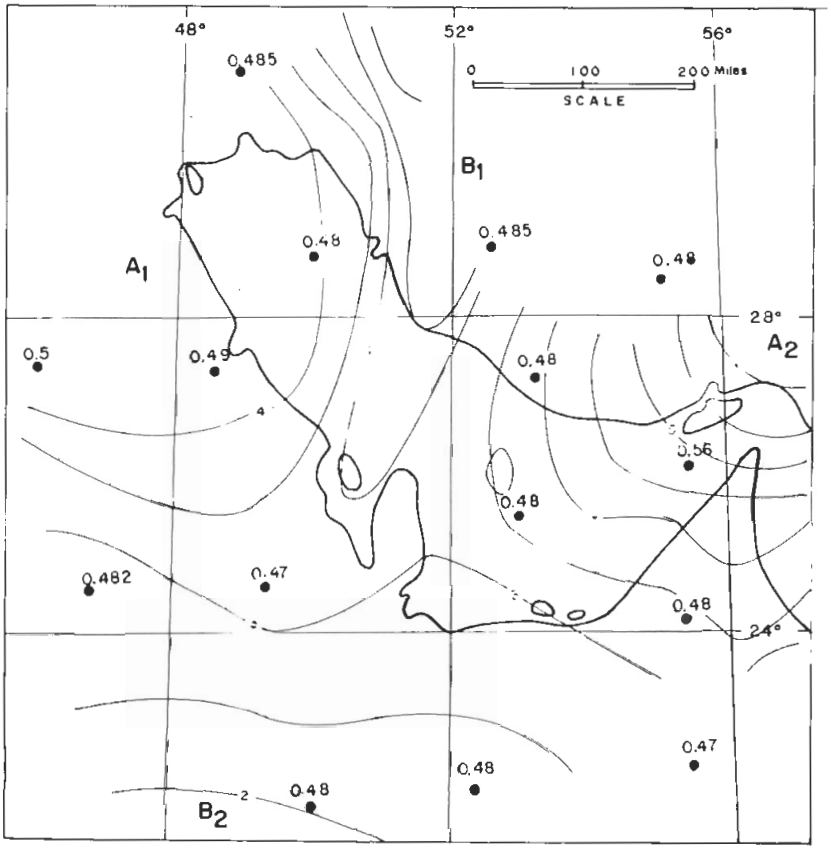

FIG. 9. Burial map of base of Permian at end of Triassic period. Refer to caption of Fig. 8 for other explanations.

3. Burial Map of Base of Permian at end of Jurassic Period (Fig. 10)

a. Sedimentation and Paleostructure

The accumulated sedimentary burial of base of Permian to the end of the Jurassic period had maximum thickness of about 8,000 ft. at the center of the geosynclines (A_1 and A_2 in Fig. 10). These thickest areas existed in the northern and eastern parts of the region. The thinnest sedimentation occurred in the nothern and southern parts of the region (B_1 and B_2 in Fig. 10).

The structural features mostly indicate the continuation of subsidences and relative uplifts in the same manner as observed previously.

b. Petroleum Generation and Maturation

The areas of the thickest sedimentary columns (maximum geosynclines) mostly show good chance for oil generation; the calculated vitrinite reflectance, R_o, ranges between 0.6 and 0.74%. On the contrary, the areas of thin sedimentation had no chance for significant oil generation (R_o<0.6%).

Note that oil is expected to be generated where vitrinite reflectance, R_o, ranges between 0.6 and 1.0% (within this range, the peak rate of oil generation may be attained between 0.75 and 0.85%, R_o). For the zone of R_o greater than 1%, we expect the conversion of oil into natural gas.

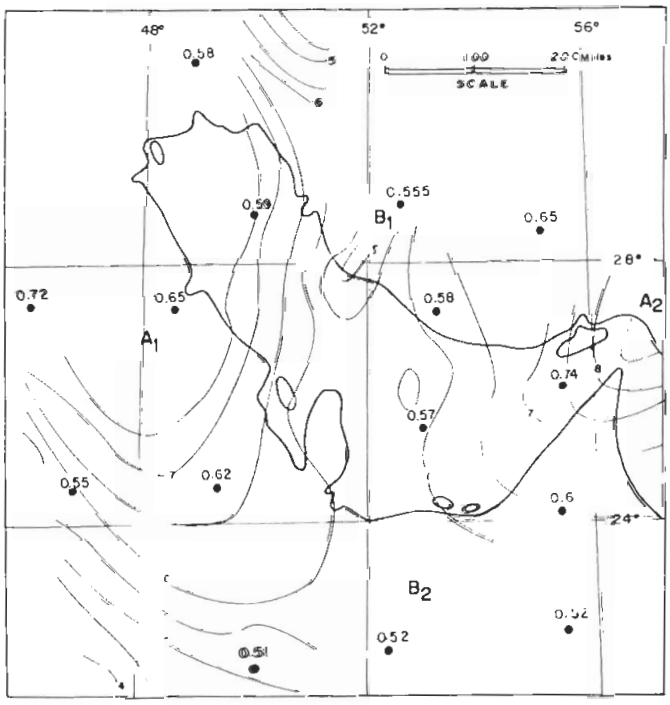

FIG. 10. Burial map of base of Permian at end of Jurassic period. Refer to caption of Fig. 8 for other explanations.

4. Burial Map of Base of Permian at end of Cretaceous Period (Fig. 11)

a. Sedimentation and Paleostructure

The burial map of the base of Permian at the end of Cretaceous shows the thickest areas in the northwestern and eastern parts of the region (A_1 and A_2 in Fig. 7). The thinnest sedimentation occurred in the northern, southern, and southwestern parts of the studied area (B_1, B_2 and B_3 in Fig. 11).

The general structural feature was not changed; both subsidence and uplift continued in similar manners from Permian to the end of Cretaceous.

b. Petroleum Generation and Maturation

Actually, the calculated vitrinite reflectance, R_o, ranges from 0.78 to 1.3%. These values suggest that the thinnest areas had best chance for oil generation (R_o<1%), whereas the geosynclines had good chance to generate wet gas through thermal cracking of oil.

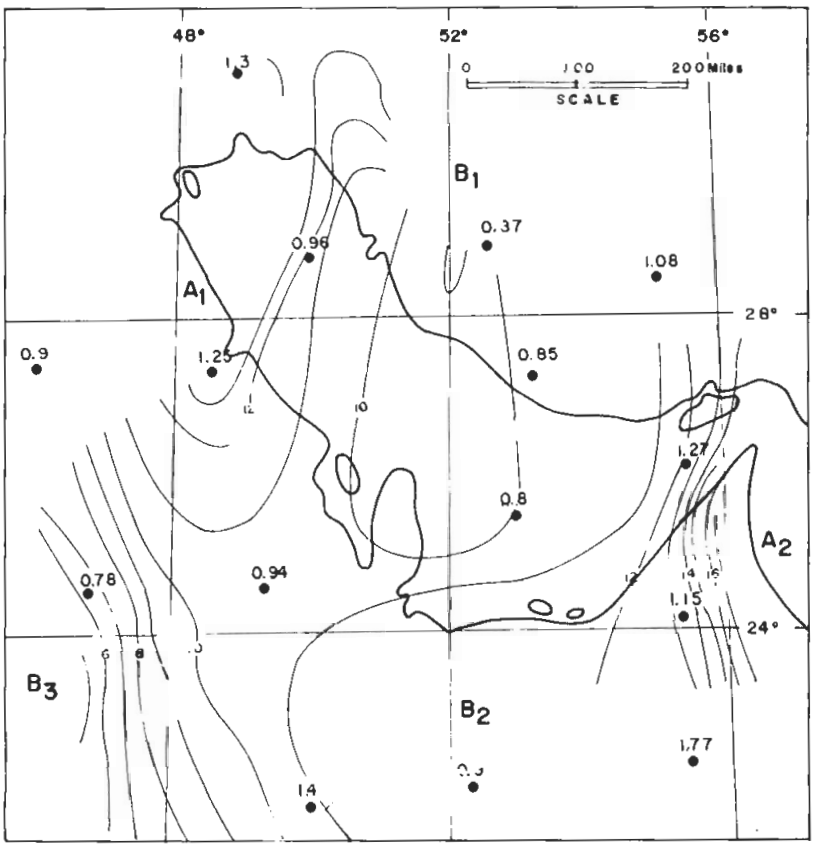

FIG. 11. Burial map of base of Permian at end of Cretaceous period. Refer to caption of Fig. 8 for other explanations.

5. Burial Map of Base of Permian at Present (Fig. 12)

a. Sedimentation and Paleostructure

The sedimentation at this burial stage is very thick in the northeastern areas (A_1 in Fig. 12), which trends from northwest to southeast. Its maximum thickness was not determined, but probably amount to about 24,000 ft. This geosyncline is known to represent the foothills of the Zagros Mountain range.

The second thickest area, which trends north-south, occurred in the eastern part of the region, where the maximum thickness is about 22,000 ft. (A_2 in Fig. 12). This geosyncline belongs to the foothills of the Oman Mountains.

The thinnest areas existed at the northern, southwestern, eastern, and central parts of the region (B_1, B_2, B_3 and B_4 in Fig. 12). The general structural feature was completely changed during Tertiary; the geosyncline had been shifted to new elongated one trending in the northwest-southeast direction. During this period, the Arabian Gulf area had been affected by thick deposition and the regional orogeny (mostly Alpine).

The compaction fluids had chances to migrate from the maximum geosynclines to their margins.

b. Petroleum Generation and Maturation

The study of petroleum generation and maturation within this period is of great importance, because it can be related to the present hydrocarbon habitats and occurrences in the Arabian Gulf region.

The calculated vitrinite reflectance, R_0, ranges between 0.98% and 4.00% in most parts. Based on Waples' (1980) definition of petroleum generation stages, four zones (major oil generation, oil and wet gas generation, wet and dry gas generation, and dry gas generation) were identified and are shown in Fig. 12.

The zone of vitrinite reflectance, R_0, between 0.98 and 1.0%, exists in the southwestern part of the region as an elongated strip (Fig. 12). This area indicates significant generation of oil.

The next zone, where R_0 ranges from 1.0 to 1.3%, occurs in the southwestern part of the region parallel to the previous area. The same maturation zone in the central part of the region has a circular pattern. Oil and wet gas are expected to exist in this zone.

The third zone has vitrinite reflectance, R_0, between 1.3 and 2.2%. It occurs in the central part of the region as a dominant feature. Both wet and dry gases are believed to have been generated from this zone.

The fourth zone has vitrinite reflectance, R_0, from 2.2 to 4.0%. It occurs along and around the geosynclines at the northeastern and eastern parts of the region. This area has the maximum thickness in the region (>24,000 ft), where only dry gas can be expected to have been generated and preserved.

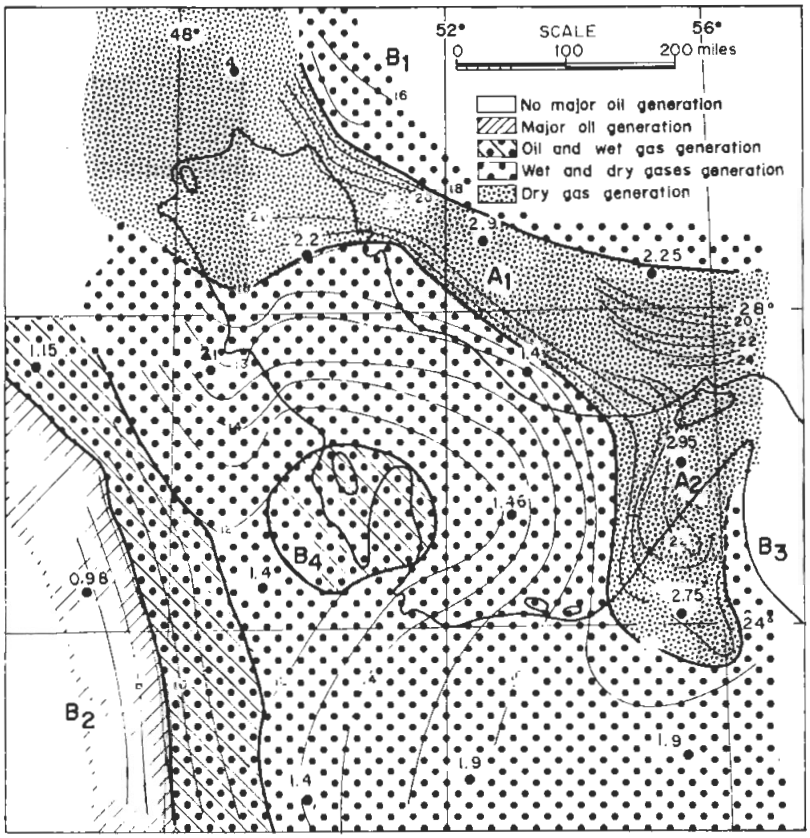

FIG. 12. Burial map of base of Permian at present. Refer to caption of Fig. 8 for other explanations.

6. *Conclusion*

In the rock of suitable organic matter within the Permian section, oil is expected to have been generated and preserved only in the areas of relatively thin deposition, whereas gases (both wet and dry) would have been dominated in most other areas. Therefore, the Permian sediments are not considered as prime source rock for the accumulated hydrocarbons in the Arabian Gulf region. There is a high probability of finding natural gas in the Permian sections. Suitability of the sediments for such gas generation is outside the scope of this study, because of lack of data, particularly in synclinal areas.

Burial and Petroleum Generation of a Bed at Triassic Base

1. Burial Map of Base of Triassic at end of Triassic Period (Fig. 13)

a. Sedimentation and Paleostructure

The sedimentation during the Triassic Period was thicknest in the northwestern and eastern parts of the Arabian Gulf region (A_1 and A_2 in Fig. 13), whereas the thinnest sedimentation existed in the northern, central, and southwestern parts of the region (B_1, B_2 and B_3 in Fig. 13).

b. Petroleum Generation and Maturation

The vitrinite reflectance, R_o, at this stage, ranges between 0.41 and 0.46%. These values indicate that there was no chance for major oil generation.

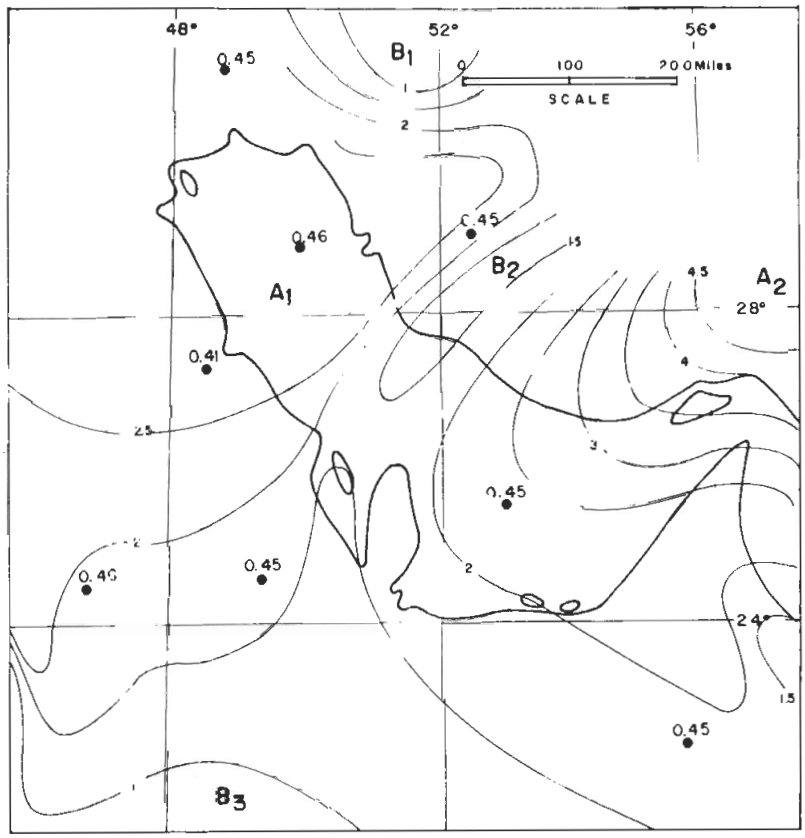

FIG. 13. Burial map of base of Triassic at end of Triassic period. Refer to caption of Fig. 8 for other explanations.

2. Burial Map of Base of Triassic at end of Jurassic Period (Fig. 14)

a. Sedimentation and Paleostructure

Figure 14 shows the burial depth of the base of Triassic at the end of Jurassic. The maximum geosynclines occurred in the northwestern and eastern parts of the region (A_1 and A_2 in Fig. 14), whereas the thinnest sedimentations existed in the northern, central, southeastern, and southwestern parts of the region (B_1, B_2, B_3 and B_4 in Fig. 14). The general structural features suggests that similar subsiding and uplifting conditions continued throughout the Triassic and Jurassic ages.

b. Petroleum Generation and Maturation

The calculated vitrinite reflectance, R_o, ranges between 0.43 and 0.57%. These values suggest that no chance for the major oil generation.

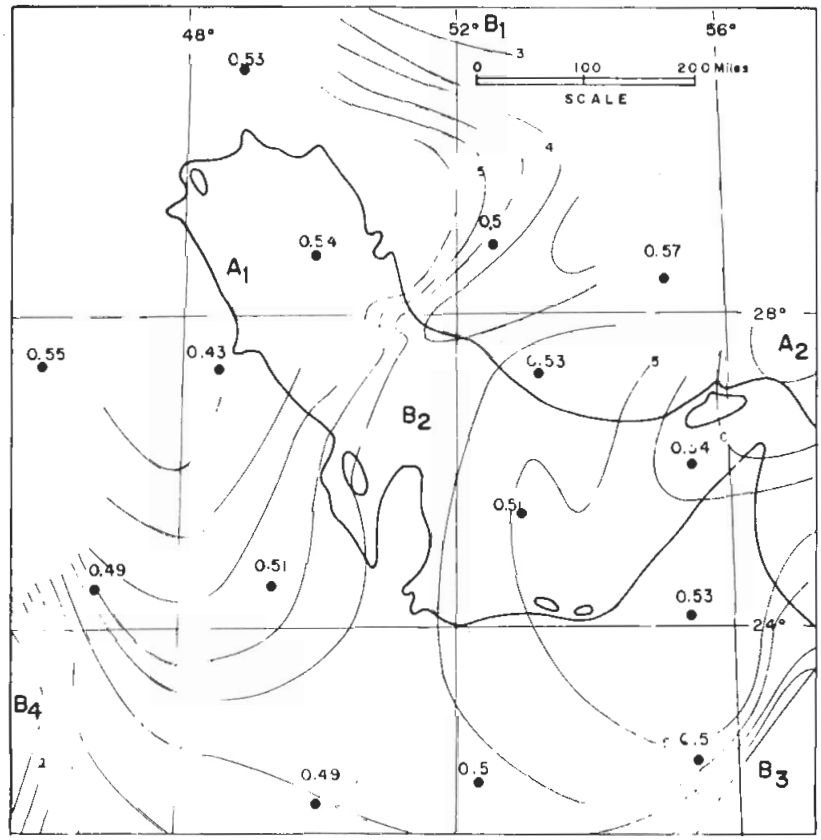

FIG. 14. Burial map of base of Triassic at end of Jurassic period. Refer to caption of Fig. 8 for other explanations.

3. Burial Map of Base of Triassic at end of Cretaceous Period (Fig. 15)

a. Sedimentation and Paleostructure

At this stage, the maximum geosynclines occurred in the northern, southeastern and northwestern parts of the Arabian Gulf region (A_1, A_2, and A_3 in Fig. 15), whereas relatively shallow burial existed in the central, southeastern and southwestern parts of the region (B_1, B_2 and B_3 in Fig. 15). There was no significant change in the general structural feature since the previous periods.

b. Petroleum Generation and Maturation

The calculated vitrinite reflectance, R_o, varies between 0.6 and 0.93%. This suggests good chance for oil generation, especially within the geosynclines.

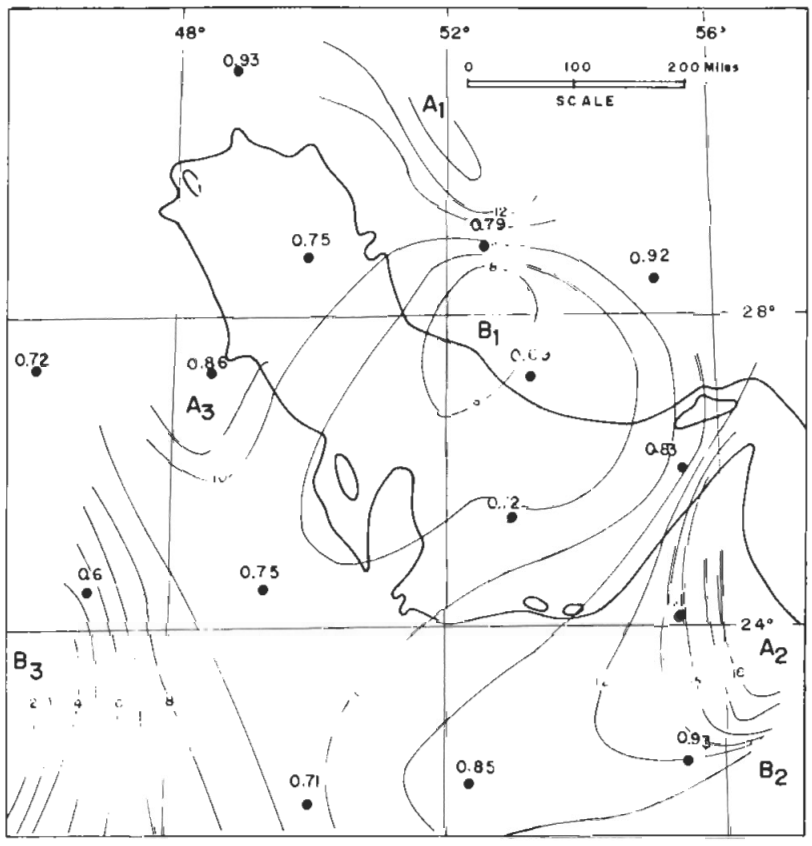

FIG. 15. Burial map of base of Triassic at end of Cretaceous period. Refer to caption of Fig. 8 for other explanations.

4. *Burial Map of Base of Triassic at Present (Fig. 16)*

a. Sedimentation and Paleostructure

Figure 16 represents the burial depth of the base of Triassic at present. The maximum geosynclines exist in the northeastern and eastern parts of the region (A_1 and A_2 in Fig. 16). The northeastern part (A_1) belongs to the foothills of the Zagros Mountains. Another geosyncline at A_2 in Fig. 16 belongs to the foothills of the Oman Mountains. On the other hand, the relatively shallow burial occurs in the northeastern, and southwestern parts of the region (B_1, B_2 and B_3 in Fig. 16). Similar subsiding and uplifting conditions continued extensively during the Tertiary period.

b. Petroleum Generation and Maturation

The vitrinite reflectance, R_o, ranges between 0.8% in the areas of shallow burial and 3.3% within the central geosyncline (Fig. 16). Four oil generation zones could be

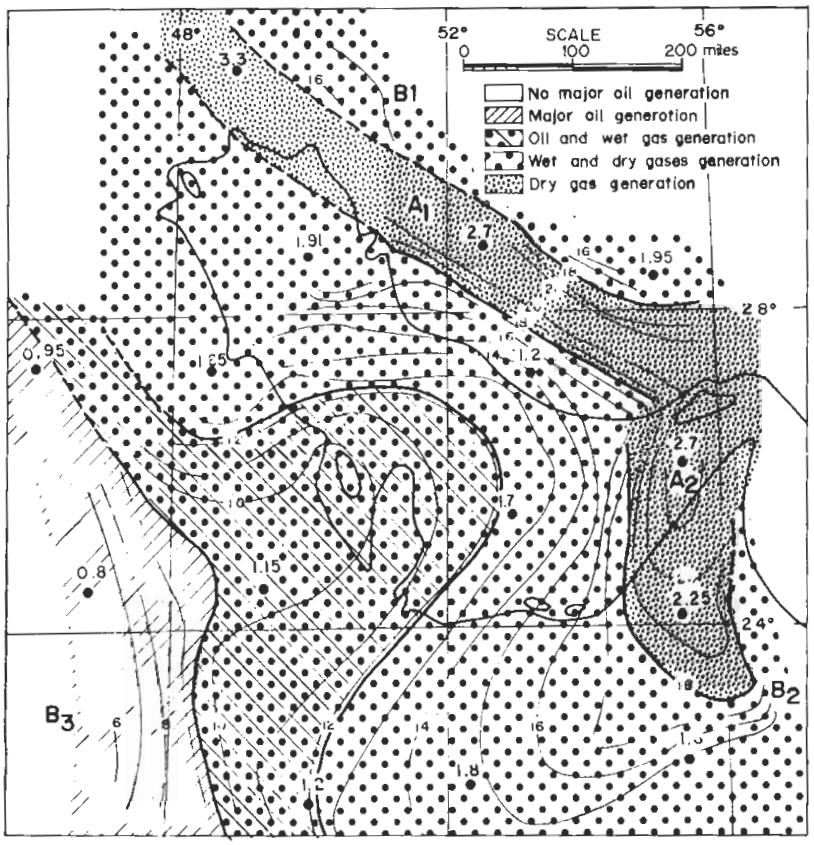

FIG. 16. Burial map of base of Triassic at present. Refer to caption of Fig. 8 for other explanations.

identified. The first zone has vitrinite reflectance, R_o, from 0.8 to 1.0%. It occurs in the northwestern part of the region with nearly north-south trend. This zone is believed to have generated only oil. The second zone has vitrinite reflectance, R_o, ranging from 1 to 1.3%. It exists in the central part of the region. This zone is expected to contain both oil and wet gas.

The third zone has vitrinite reflectance, R_o, ranging between 1.3 and 2.2% which occurs in the northeastern, southeastern, southern, and western parts and extends to the central part of the region. Within this zone, both wet and dry gases are expected to have been generated and preserved to the maximum depth of about 18,000 ft. The fourth zone has vitrinite reflectance, R_o, between 2.2 and 4.8%. It occurs in the northeastern parts of the region. In this zone, only dry gas is expected to have been generated and preserved.

5. Conclusions

Actually, the gas generation dominates in the region, whereas oil generation zone occurs in the areas of relatively shallow burial. This suggests that the Triassic sediments may be good source rocks for gas, but not for oil within the Arabian Gulf region. Again, the suitability of the sediments for gas generation is outside the scope of this paper.

Burial and Petroleum Generation of a Bed at Jurassic Base

1. Burial Map of Base of Jurassic at end of Jurassic Period (Fig. 17)

a. Sedimentation and Paleostructure

The sedimentation during the Jurassic period was spread over the entire Arabian Gulf region (Fig. 17). Generally, the region had the maximum geosyncline in the western part (A_1 in Fig. 17). The thinnest sedimentation occurred in the northeastern, southeastern and southwestern parts of the region (B_1, B_2 and B_3 in Fig. 17).

b. Petroleum Generation and Maturation

Here, the vitrinite reflectance, R_o, varies from 0.45 to 0.49%, suggesting that there was no chance for the major oil generation at this stage.

2. Burial Map of Base of Jurassic at end of Cretaceous (Fig. 18)

a. Sedimentation and Paleostructure

The maximum geosyncline occurred in the northwestern, northern, and southeastern parts of the region (A_1, A_2 and A_3 in Fig. 18), whereas the thinnest sedimentation occurred in the northern, central, southeastern and southwestern parts of the region (B_1, B_2, B_3 and B_4 in Fig. 14). During this period, the region had probably been af-

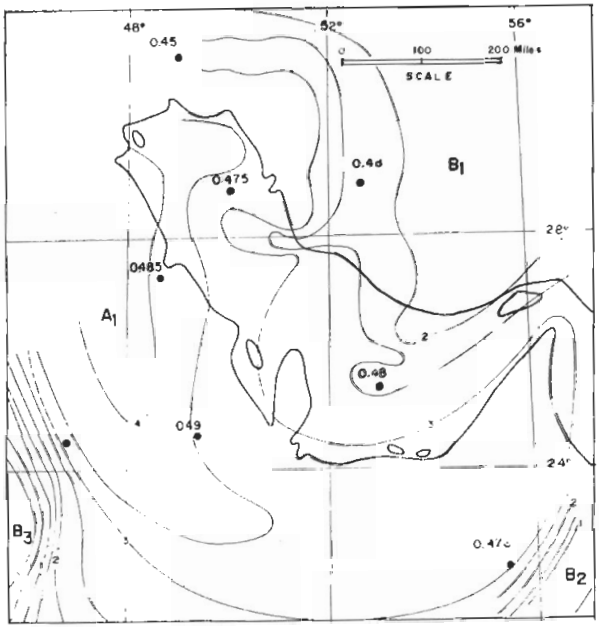

FIG. 17. Burial map of base of Jurassic at end of Jurassic period. Refer to caption of Fig. 8 for other explanations.

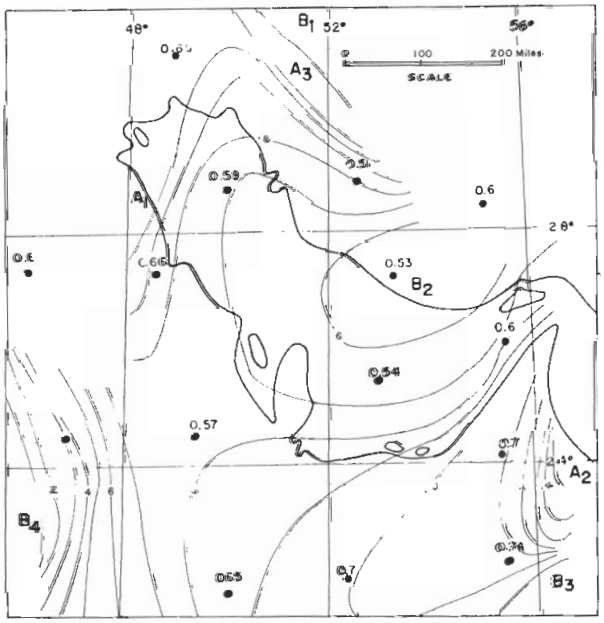

FIG. 18. Burial map of base of Jurassic at end of Cretaceous period. Refer to caption of Fig. 8 for other explanations.

fected by subsidence (A_1, A_2 and A_3 in Fig. 14) and relative uplift (B_1, B_2, B_3 and B_4 in Fig. 18). The foothills of Iran and Oman had been formed during this period (A_2 and A_3 in Fig. 18).

b. Petroleum Generation and Maturation

The calculated vitrinite reflectance, R_o, ranges between 0.54 and 0.74%. Oil is expected to have been generated in the maximum geosynclines (R_o>0.6%), especially in the southeastern one (A_2 in Fig. 18), if there were suitable source rocks. There was no chance for major oil generation in the relatively shallow burial areas.

3. *Burial Map of Base of Jurassic at Present (Fig. 19)*

a. Sedimentation and Paleostructure

Figure 19 shows the burial depth of the base of the Jurassic formations at present. The maximum geosynclines occur in the northeastern and eastern parts of the region (A_1 and A_2 in Fig. 19), whereas the thinnest sedimentation existed in the northeastern, southeastern, central and southwestern parts of the region (B_1, B_2, B_3 and B_4 in Fig. 19).

The general structural feature was completely changed in the northeastern geosyncline during the Tertiary period (A_1 in Fig. 19). It belongs to the foothills of the Zagros Mountains in Iran. The geosyncline shown as A_2 in Fig. 19 suggests that subsidence similar to the one in A_1 continued in a relatively small area in Oman. In summary, it may be stated that the foothills of the Zagros and Oman Mountains were formed since Cretaceous.

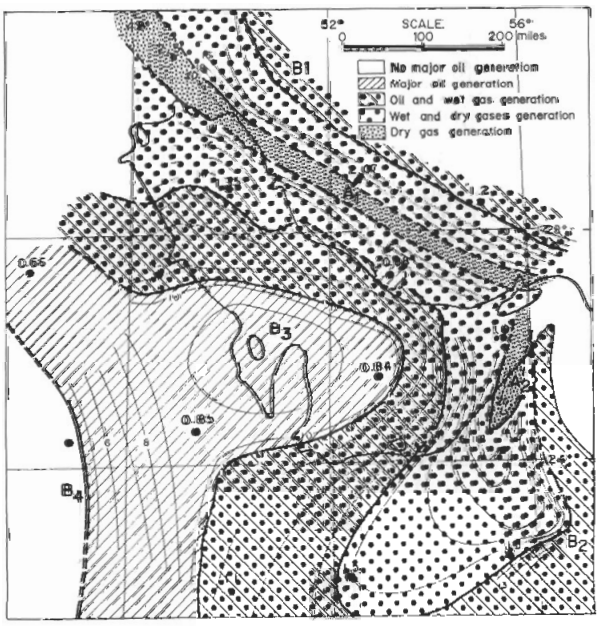

FIG. 19. Burial map of base of Jurassic at present. Refer to caption of Fig. 8 for other explanations.

b. Petroleum Generation and Maturation

The vitrinite reflectance, R_o, varies between 0.66 and 2.5%. Four oil generation and maturation zones are identified (Fig. 19). The first maturation zone, with vitrinite reflectance, R_o, values between 0.66 and 1.0%, occurs in the southwestern and central parts of the region. This zone is believed to have generated oil in significant amounts, if there are suitable source rocks.

The next maturation zone, with vitrinite reflectance, R_o, between 1.0 and 1.3%, occurs in the southeastern, eastern, central, and northwestern parts of the region. Most oils were being converted to wet gas within this zone.

The third maturation zone which has vitrinite reflectance, R_o, between 1.3 and 2.2%, exists in the northeastern and eastern parts of the region. Wet and dry gases are expected to have been generated in this late stage of the burial depth of about 18,500 ft. The vitrinite reflectance, R_o, in the fourth maturation zone ranges from 2.2 to 2.5%. It occurs in a small area in the northern part of the region where only dry gas can be expected.

4. Conclusion

Figure 19 suggests a possibility of oil generation in the Jurassic formations in the southwestern and central parts of the region. On the other hand, the Jurassic sedimentary rocks in most other parts of the region has reached the stages of over maturation for oil. Only wet and dry gases can be expected from these source rocks. Suitability of the Jurassic sediments for generating oil will be discussed later.

Burial and Petroleum Generation of a Bed at Cretaceous Base

1. Burial Map of Base of Cretaceous at end of Cretaceous (Fig. 20)

a. Sedimentation and Paleostructure

Sedimentation during the Cretaceous period caused its maximum burial in the northeastern, southeastern, and western parts of the region (A_1, A_2 and A_3 in Fig. 20). The northeastern geosyncline had been elongated in the northwest-southeast trend, which belongs to the foothills of the Zagros Mountains, whereas the southeastern trend belongs to foothills of Oman (A_1 and A_2 in Fig. 20). The thinnest sedimendation occurred in the northeastern, southeastern, central, and southwestern parts of the region (B_1, B_2, B_3 and B_4 in Fig. 20).

b. Petroleum Generation and Maturation

The calculated vitrinite reflectance, R_o, ranges between 0.47 and 0.72%. It suggests that there was a good chance for oil generation around the southeastern geosyncline (A_2 in Fig. 20). However, the other parts of the region did not reach a significant oil generation stage.

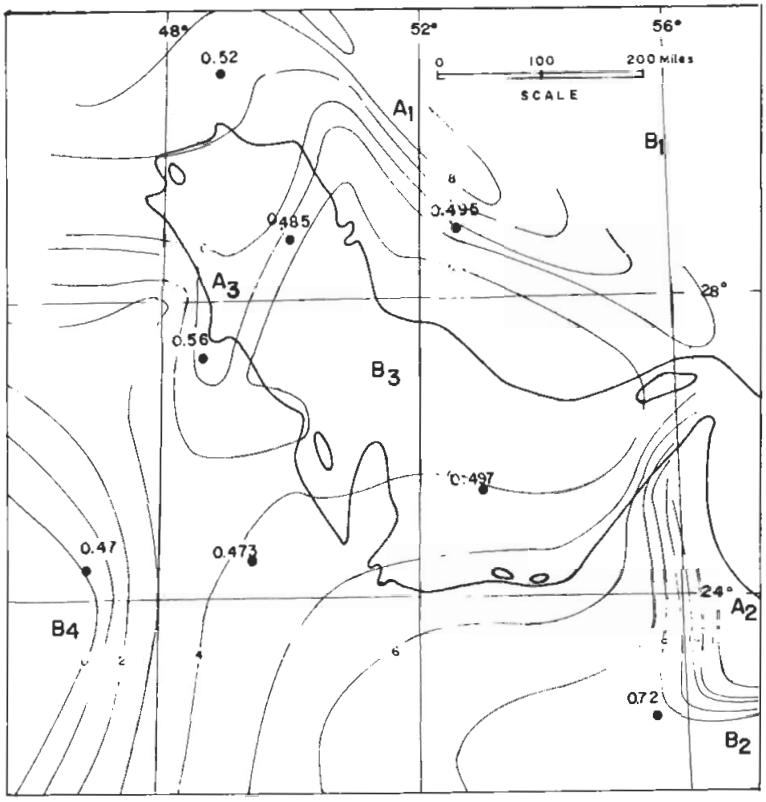

FIG. 20. Burial map of base of Cretaceous at end of Cretaceous period. Refer to caption of Fig. 8 for other explanations.

2. *Burial Map of Base of Cretaceous at Present (Fig. 21)*

a. Sedimentation and Paleostructure

Figure 21 shows the burial map of base of the Cretaceous formations at present. The thickest sedimentation occurs in the northeastern and east-southeastern parts of the region (A_1 and A_2 in Fig. 21), whereas the thinnest sedimentation occurred in the northern, southeastern, central, and northwestern parts of the region (B_1, B_2, B_3 and B_4 in Fig. 21). Both Fig. 20 and 21 suggest that similar subsiding and relative uplifting features continued throughout Cretaceous and Tertiary periods.

b. Petroleum Generation and Maturation

The calculated vitrinite reflectance, R_o, ranges between 0.5 and 1.8%. Three petroleum generation and maturation zones are identified (Fig. 21). The first maturation zone has vitrinite reflectance, R_o, between 0.5 and 0.6%, which occurs in the southwestern part and is extending to the central parts of the region with maximum depth of about 6,100 ft. This zone shows no chance for a major oil generation.

The second maturation zone which has vitrinite reflectance, R_0, from 0.6 to 1.0%, occurs in the northwestern, central, eastern, and southeastern parts of the region. The maximum depth amounts to about 11,200 ft. This zone suggests oil generation and preservation in significant amounts, if there are proper source rocks.

The third maturation zone has vitrinite reflectance, R_0, between 1.0 and 1.3%. It exists in the northeastern, eastern, and southeastern parts of the region within the geosynclines. This zone is expected to have generated and preserved wet gas from oil. In other words, it suggests a possible existence of both oil and wet gas in this zone.

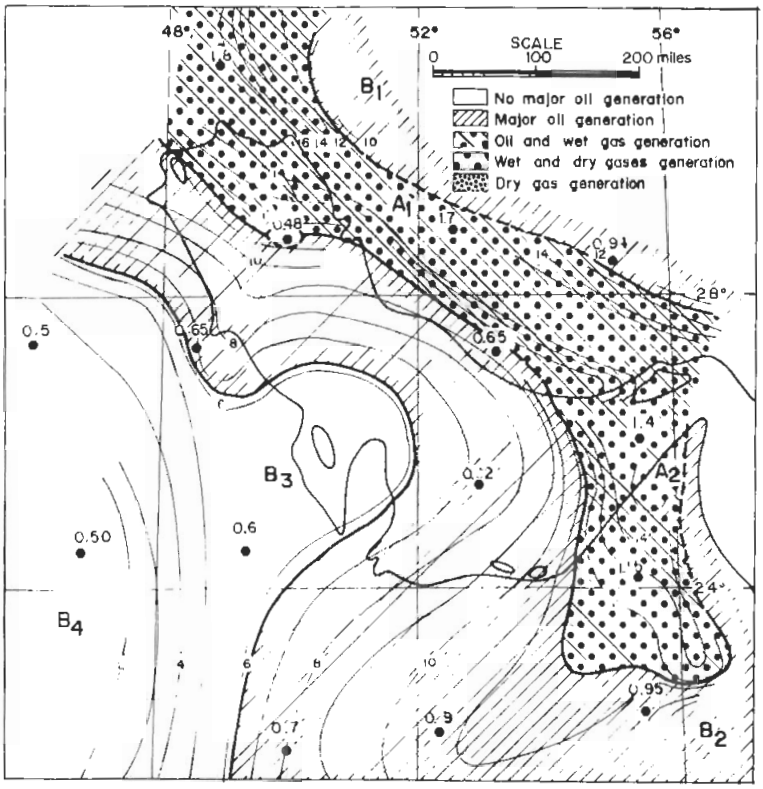

Fig. 21. Burial map of base of Cretaceous at present. Refer to caption of Fig. 8 for other explanations.

3. Conclusion

The major oil generation and maturation zone within the Cretaceous sediments suggests a possibility of the existence of mature source rocks for the accumulated hydrocarbons in the northwestern, central, southern, and southwestern parts of the region. The western and central parts have, however, no chance to generate a significant amount of oil. Wet gas may have generated in the over-matured zone along the geosynclines in the region.

Suitable source section of Cretaceous will be described later.

Burial and Petroleum Generation of a Bed at Tertiary Base

1. *Burial Map of Base of Tertiary at Present (Fig. 22)*

a. Sedimentation and Paleostructure

The thickest sedimentation occurs in the northeastern and east-southeastern parts of the region (A_1 and A_2 in Fig. 22), whereas the thinnest sedimentation exists in the northeastern, southeastern, southwestern, and central parts of the region (B_1, B_2, B_3 and B_4 in Fig. 22).

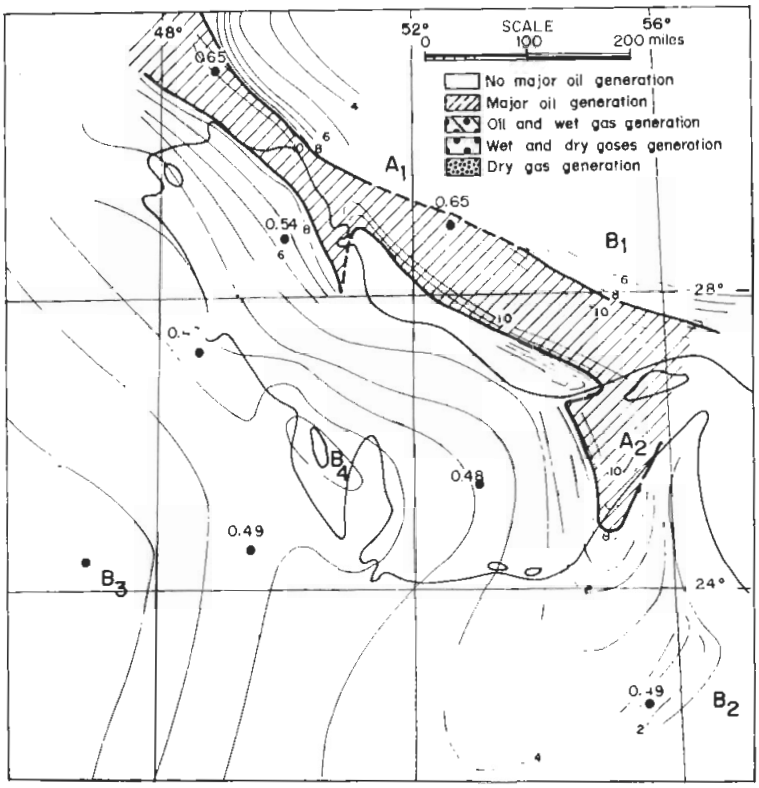

FIG. 22. Burial map of base of Tertiary at present. Refer to caption of Fig. 8 for other explanations.

b. Petroleum Generation and Maturation

The vitrinite reflectance, R_o, ranges between 0.47 and 0.68%. The immature zone, which has vitrinite reflectance, R_o, between 0.46 and 0.6%, occurs throughout the region except the geosynclines. This zone has no chance for major oil generation.

The maturation zone in Fig. 22 has vitrinite reflectance, R_o, between 0.6 and 0.68%. It exists in the northeastern and eastern parts of the region along the

geosynclines. This zone is expected to have generated at least heavy oil, if there are suitable source rocks.

2. Conclusion

The oil generation zone within the Tertiary sediments occurs only in the foothills of the Zagros and Oman mountains, whereas the other parts of the region are still immature.

Probable Source Rocks in Jurassic and Cretaceous Formations in Saudi Arabia

Data on the source rocks, in general, are scarce in this region. Ayres *et al.* (1982) reported the probable source rocks of the Jurassic and Cretaceous ages in Saudi Arabia. Figure 23 shows the summary of their observation; 1. there are several source sections in Jurassic such as those of the Marrat, Dhruma and Twaiq Mountain-Hanifa Formations, 2. there is a major source section in the basal part of the Cretaceous section (Sulaiy).

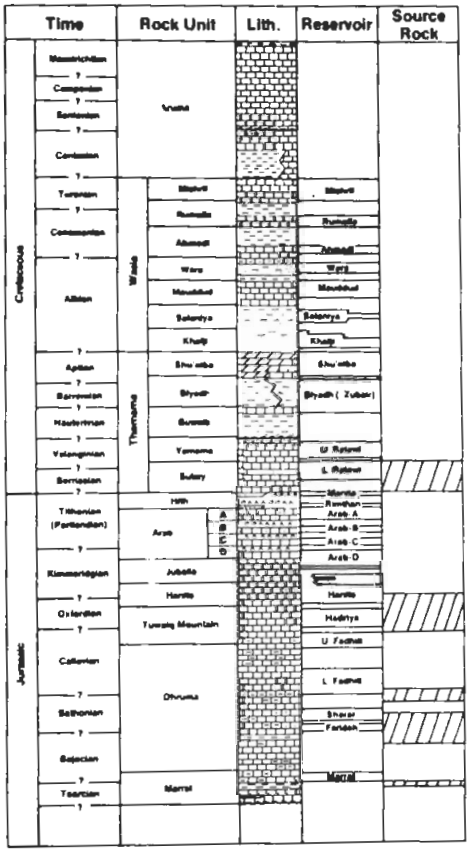

FIG. 23. Generalized Cretaceous and Jurassic stratigraphic section showing lithology, reservoir units, and source rocks (from Ayres *et al.* 1982).

For the other geologic formations (Permian, Triassic and Tertiary), there is no reliable source rock data on a regional basis.

Superposition of Oil Field Distribution Over Oil Generation Map

In order to evaluate the applicability of the oil generation maps for exploration, it would be interesting and worthwhile to compare these maps with the actual distribution of oil fields in the Arabian Gulf region. This is particularly true for the Jurassic, Cretaceous and Tertiary formations which contain significant amounts of oil.

Figure 24 shows such a map of superpositions for Jurassic; this figure suggests that some of the oils trapped in the formations of this age (mostly Upper Jurassic) derived from the source rocks of the basal Jurassic formations. However, some oil fields occur in the over-mature zone of the basal Jurassic. This further suggests that oil may have derived from the source rocks of the Middle Jurassic formations as well. Note that, according to Ayres *et al.* (1982), there is no major source sections in the Upper part of the Jurassic Formations.

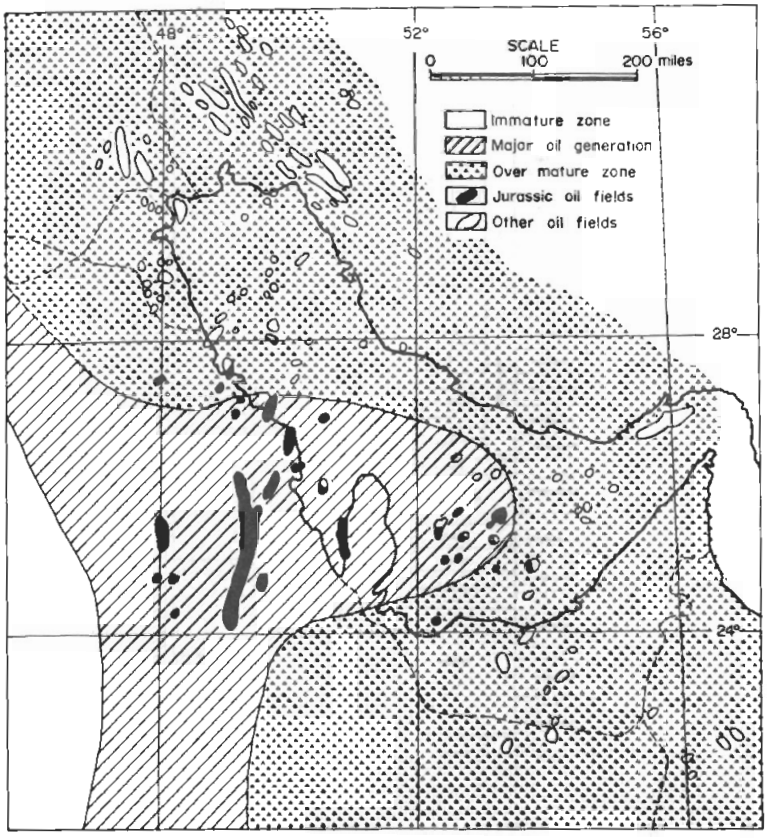

FIG. 24. Map of Jurassic oil generation zone and Jurassic producing oil fields.

Figure 25, on the other hand, depicts a similar map for the Cretaceous formations. There is generally a good match between the oil field distribution and maturation zone, except the field at Bahrain where the area is generally immature. The structure in Bahrain is an anticline, probably associated with deep-seated salt growths. The oil may have migrated upward from the Jurassic source rocks to the Cretaceous reservoirs through faults and fractures caused by the salt growths.

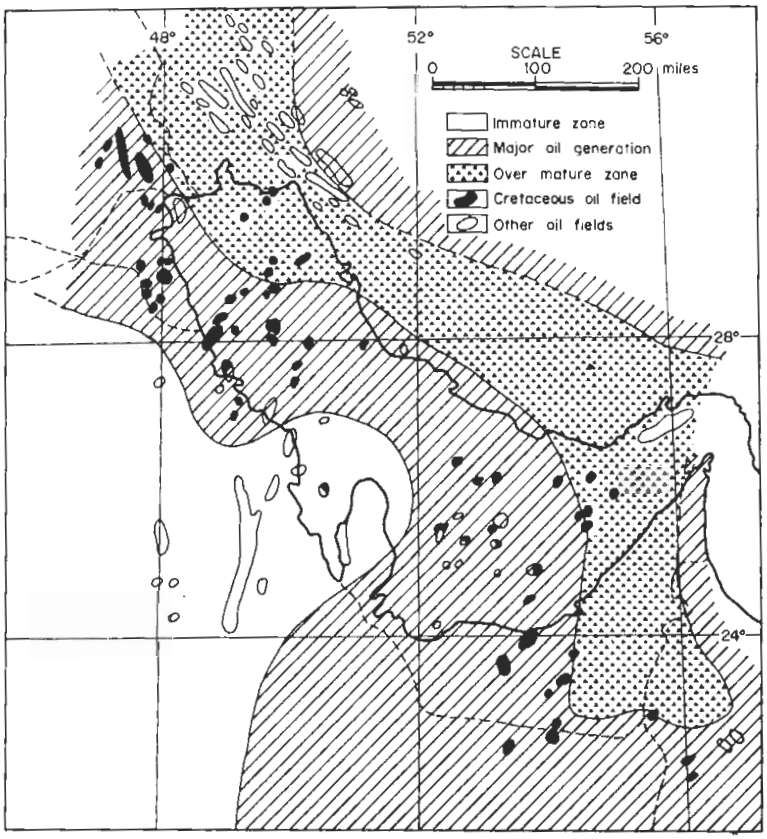

FIG. 25. Map of Cretaceous oil generation zone and Cretaceous producing oil fields.

The comparison between the Tertiary oil field distribution and source rock maturation could be seen in Fig. 26. The Tertiary mature zone exists in the eastern and northwestern parts of the region, whereas the main producing oil fields occur in the northwestern part. Many oil fields occur in the immature zone, where significant vertical migration of oil from the Cretaceous source rocks may have taken place. Based on their independent study of ages of accumulated oils and reservoirs, Young *et al.* (1977) also suggested such a possibility of long-distance vertical migration of oil in this region.

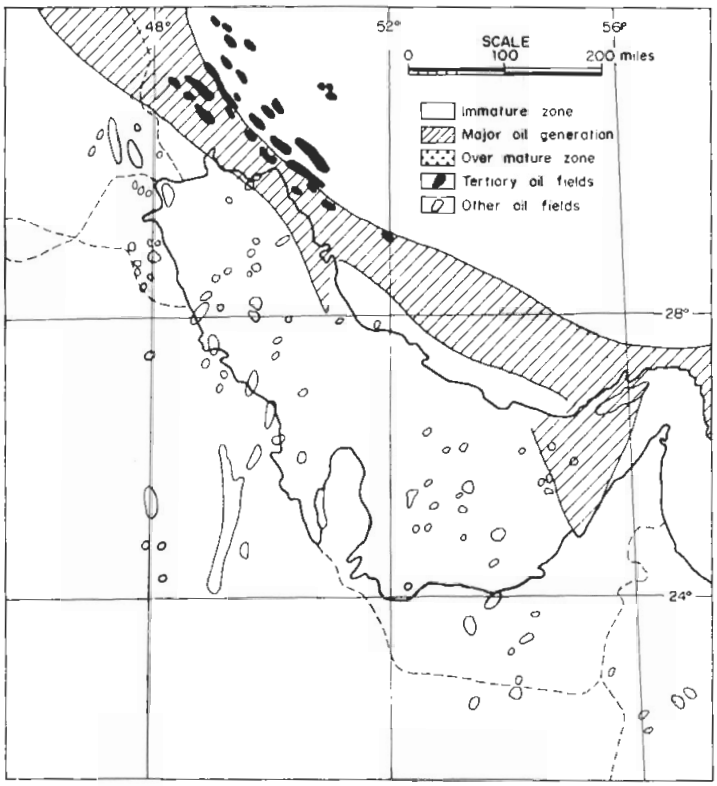

FIG. 26. Map of Tertiary oil generation zone and Tertiary producing oil fields.

Conclusions

There are two main conclusions from the current study. Each of them could be described in detail as follows:

1. The application of Lopatin's and Waples' methods for petroleum generation and maturation suggests the following:
   - The Permian and Triassic sedimentary rocks are possible sources mainly for gas.
   - The Tertiary sediments may be source of immature heavy oils.
   - The Jurassic and Cretaceous sedimentary rocks are the main source for oil in the region.

2. The superposition of the Jurassic, Cretaceous and Tertiary oil generation and maturation zones over the existing oil fields suggests the following:
   - The Jurassic sedimentary rocks would have generated the oils accumulated in the Jurassic producing oil fields. Source rocks in the basal and middle parts of Jurassic are the most important in this respect.
   - The Cretaceous sedimentary rocks have generated the oils accumulated in the Cretaceous and Tertiary producing oil fields.

References

Ala, M.A. (1982) Chronology of trap formation and migration of hydrocarbons in Zagros section of Southwest Iran, *AAPG Bull.* **66**(10): 1535-1541.

Ayres, M.G., Bital, M., Jones, R.W., Slentz, L.W., Tarter, M. and **Wilson, A.O.** (1982) Hydrocarbon habitat in main producing areas, Saudi Arabia, *AAPG Bull.* **66** (1): 1-9.

Beydoun, Z.K. and **Dunnington, H.V.** (1975) *Petroleum Geology and Resources of the Middle East*, Scientific Press Ltd., Beacons Field, Bucks, U.K., 99 p.

Connan, J. (1974) Time-temperature relations in oil genesis, *AAPG Bull.* **58:** 2516-21.

Dow, W.G. (1977) Kerogen studies and geological interpretations, *J. Geochem. Explor.* **7:**79-99.

Dow, W.G. (1978) Petroleum source beds on continental slopes and rises, *AAPG Bull.* **62:**1584-1606.

Kamen-Kaye, M. (1970) Geology and productivity of Persian Gulf Synclinorium, *AAPG Bull.* **54**(12): 2371-2394.

Lopatin, N.V. (1971) Temperature and geologic time as factors in coalification (In Russian), *Akad Nauk SSSR IXV. Ser. Geol* no. 3: 95-106.

Murris, R.J. (1980) Middle east, stratigraphic evolution and oil habitat, *AAPG Bull.* **64:** 597-618.

Powers, R.W., Ramirez, L.F., Redmond, C.D. and **Elberg, E.L.** (1966) Geology of the Arabian Peninsula, Sedimentary Geology of Saudi Arabia, *U.S. Geol. Survey Prof. Paper*, **560-D,** 127 p.

Waples, D.W. (1980) Time and temperature in petroleum formation: Application of Lopatin's method to petroleum exploration, *AAPG Bull.* **64:** 916-926.

Young, A., Monaghan, P.H. and **Schweisberger, R.T.** (1977) Calculation of ages of hydrocarbons in oils-physical chemistry applied to petroleum geochemistry, *AAPG Bull.* **61**(4): 572-600.

منشأة البترول ونضوجه في منطقة الخليج العربي

إبراهيم السيل وكنجي ماجارا
كلية علوم الأرض – جامعة الملك عبد العزيز
جدة – المملكة العربية السعودية

أثبتت نتائج تطبيق واستخدام طرق كل من لوباتان ووابلز لدراسة نشوء ونضوج البترول في منطقة الخليج العربي أن الصخور الرسوبية لعصري البرمي والترياسي للمصادر المحتملة للغاز فقط ، وأن رواسب الترياسي الثلاثي تنتج فقط النفط الثقيل (غير الناضج) . كما أن دراسة صخور المصدر للعصر الجوراسي والطباشيري تدل على كونها المناشيء الرئيسية للهيدروكربونات ذات الانتشار الاقليمي الواسع .

كما أن توافق وتراكب حقول الزيت والغاز الموجودة مع خرائط نشوء البترول تؤكد النتائج السابقة وتدعمها .